DEVELOPMENT AND COMPARATIVE STUDY ON THE MECHANICAL PROPERTIES OF ALUMINA-SILICON CARBIDE AND BORON CARBIDE CERAMIC AS MATERIALS FOR BALLISTIC APPLICATION

Audu, M.U., Akindapo, J.O. and Orueri, D.U.*

Mechanical Engineering Department, Nigerian Defence Academy

*Corresponding email: danielorueri@nda.edu.ng

ABSTRACT

This study addresses the challenge of developing lightweight, high-performance composite materials for ballistic and protective applications, as current solutions often face trade-offs between stiffness, strength, and energy absorption. The aim of this research was to investigate and compare the mechanical properties of Alumina-Silicon Carbide (Al_2O_3-SiC) and Alumina-Boron Carbide (Al_2O_3-B_4C) composites to determine their suitability for ballistic and high-performance uses. Using characterization techniques such as Scanning Electron Microscopy (SEM), Energy Dispersive X-ray Spectroscopy (EDS), X-ray Diffraction (XRD), X-ray Fluorescence (XRF), and Fourier Transform Infrared Spectroscopy (FTIR), the composites' microstructural, elemental, and chemical properties were analyzed. Mechanical behavior was assessed through hardness, impact, and tensile strength tests. The results showed that Al_2O_3-SiC exhibited high stiffness (1243.80 MPa), moderate tensile strength (89.00 MPa), and low elongation, making it suitable for rigid armor applications. In contrast, Al_2O_3-B_4C demonstrated superior stiffness (1461.54 MPa), moderate tensile strength (81 MPa), and moderate ductility (4.7% elongation), indicating its suitability for medium ballistic protection and energy absorption. Based on these findings, it is recommended that Al_2O_3-SiC composites be prioritized for applications requiring hard armor with high stiffness, while Al_2O_3-B_4C composites are better suited for scenarios needing balanced protection and energy dissipation.

Keywords: Alumina-Silicon Carbide, Alumina-Boron Carbide, Ballistics, Energy Absorption, Mechanical Properties, Armour Applications

1 INTRODUCTION

In the modern world, a society's socio-economic stability is deeply intertwined with the safety of its people and critical infrastructure. National security is essential for achieving social, economic, and political goals, as no meaningful development can occur in an environment plagued by insecurity [1]. Every nation strives to uphold its core principles, ensuring its citizens can live freely and securely while preserving national identity, sovereignty, and interests. Unfortunately, Nigeria faces growing internal security challenges, with insurgencies such as Boko Haram (ISWAP) in the North-East, banditry in the North-West, and separatist movements in the South-East, among others [2, 3]. These threats underscore an urgent need for the country to develop indigenous materials for the protection of military hardware and other critical assets [3]. Ballistic impact occurs when a high-velocity projectile collides with a surface, akin to small arms fire or high-speed debris impact. Understanding how materials respond to these forces is crucial for designing effective protective systems [4, 5]. Armour, whether personal, vehicular, or structural, plays a vital role in shielding against such threats. Modern advancements in material science have led to the development of composite materials, which offer superior strength, durability, and

lightweight properties compared to conventional materials [6]. Among composite materials, Metal Matrix Composites (MMC) and Ceramic Matrix Composites (CMC) have gained significant attention for ballistic applications. CMCs, consisting of ceramic fibers embedded within a ceramic matrix, exhibit high strength, thermal stability, and improved fracture resistance. These materials address the limitations of traditional ceramics, such as brittleness and susceptibility to microcracks [7, 8]. Common CMC reinforcements include silicon carbide (SiC), alumina (Al_2O_3), and boron carbide (B_4C), which enhance toughness through crack deflection and fiber bridging mechanisms [9]. Boron carbide, one of the hardest known materials, is widely used in military and industrial applications, including bulletproof vests and armored vehicles. Aluminum oxide (Al_2O_3) and silicon carbide (SiC) are also extensively utilized in protective applications due to their high hardness, thermal resistance, and structural integrity [10, 11]. Given Nigeria's security challenges, there is a pressing need to identify suitable materials for developing ballistic armor capable of withstanding high-velocity impacts. This research focuses on formulating, evaluating, and comparing the mechanical properties of aluminum-silicon carbide and boron carbide ceramic composites. The objective is to determine the most viable candidate material for producing ballistic vehicle body armor, enhancing protection for military and security personnel while promoting local material development [12, 13].

2 LITERATURE REVIEW

Below is a summary of key research studies relevant to this work. These works provide foundational insights and frameworks that inform the current study. Medvedevski [14] conducted research on lightweight ceramic composite armor systems with an aramid backing, an intermediate lightweight ceramic-polymer layer, and a front ceramic plate. The newly proposed armor system demonstrated superior ballistic performance by effectively stopping 7.62 mm NATO Ball FMJ, 7.62 × 54R LPS, and 7.62 × 63 mm AP M2 projectiles, depending on the front ceramic plate thickness. Compared to conventional armor systems that consist of a front ceramic plate and aramid backing, the proposed design allowed for a thinner backing while improving ballistic resistance. The enhanced performance was attributed to the three-component design, particularly the intermediate layer with a specially formulated ceramic filler, which promoted surface multiplicity upon ballistic impact and increased kinetic energy absorption. This configuration effectively reduced crack propagation, particularly shock wave-induced cracks, which further eroded the projectile. Additionally, the developed armor systems were lightweight, with composite systems based on thin alumina-mullite ceramic plates reducing weight by up to 2000–2100 g while still offering multihit protection against NATO Ball and LPS ammunition. The proposed composite design has potential applications in vehicle, personnel, and structural armor systems. Halil *et al*. [15] investigated the mechanical and ballistic performance of boron carbide-reinforced Al 6061 aluminum alloy produced via powder metallurgy. The study aimed to determine the impact of ceramic content and the production process on the physical and ballistic properties of the resulting composites. The density, hardness, impact toughness, transverse rupture strength, tensile strength, and ballistic resistance of Al 6061 alloy reinforced with boron carbide (B_4C) powders were evaluated. Metal matrix composites with 5 wt.%, 10 wt.%, 15 wt.%, and 20 wt.% B_4C were fabricated using powder metallurgy and hot extrusion. Some specimens also underwent hot rolling to examine its influence on mechanical and ballistic characteristics. The results showed that all specimens exhibited high relative density values with uniform particle distribution in the matrix. However, as the volume fraction of B_4C increased, hardness, transverse rupture strength, tensile strength, and impact toughness declined for both hot-rolled and hot-extruded samples. Hotrolled composites displayed the highest tensile strength, while hot-extruded specimens exhibited the highest flexural strength. The deformation testing revealed transgranular cracking on B_4C particles and particle retention in the matrix. Olawale *et al*. [16] conducted a ballistic study on alumina-ceramic steel composite for structural applications. The composite consisted of 95.66 wt.% dry alumina powder, 2.78 wt.% PVA, 1.28 wt.% CaO, and 0.28 wt.% MgO, following an optimal material elaboration ratio from prior research. The mixture was compressed uniaxially at 110 MPa in a metallic mold (100 × 100 × 20 mm) and sintered at 1500°C for 60 minutes. The results showed that the sintered ceramic possessed competitive mechanical properties suitable for armor applications, serving as a viable alternative to commercially available sintered ceramics. Ballistic testing demonstrated that the ceramic component provided significant protection to

armor steel, delaying projectile penetration. Additionally, using a steel-ceramic-steel (S-C-S) laminate configuration was effective in stopping armor-piercing (AP) rounds when commercial medium-carbon steel was used. Furthermore, the ballistic performance of the composite could be significantly enhanced by optimizing the heat treatment process of the medium-carbon steel. Saurab *et al*. [17] examined the ballistic performance of ceramic-metal composite structures through numerical analysis. The study compared two ceramic-metal composites—one reinforced with alumina (Al_2O_3) and the other with boron carbide (B_4C)—both tested on aluminum backing plates. The round ceramic plates (101 mm diameter, 25 mm thickness) were centered on aluminum plates (152 mm diameter, 64 mm thickness). A tungsten projectile (7.62 mm diameter, 76.2 mm length) impacted the composites at 1550 m/s. The LS-DYNA solver was used for numerical simulations, validated against experimental data. The study assessed penetration depth, ballistic limit, and target area density, revealing that B_4C/Al outperformed Al_2O_3/Al by 44% in penetration resistance, 14% in ballistic limit, and area density. These results confirmed the superior ballistic resistance of boron carbide-reinforced aluminum composites. Shahid *et al*. [18] investigated the synthesis and mechanical characterization of alumina-based composite materials for armor applications. The study focused on improving toughness, a critical factor for fracture resistance. Three distinct ceramic composites were analyzed: alumina (Al_2O_3), zirconia-toughened alumina (ZTA), and alumina with silicon carbide (SiCA). Hexagonal samples were fabricated via dry pressing and sintered at 1600°C in an argon atmosphere. SEM and optical microscopy revealed fine grain size distribution in the matrix, while BSE imaging confirmed the presence of ZrO_2 particles. The SiCA samples exhibited relatively high porosity (~6.35%), as confirmed by EDX analysis. Mechanical testing showed an inverse relationship between toughness and hardness. ZTA samples displayed the highest toughness (4.6 $MPa \cdot m^{1/2}$), whereas SiCA samples had the highest hardness. The study concluded that these composite materials offer properties comparable to other ceramic armor materials manufactured through different techniques.

3 MATERIALS AND METHODS

3.1 Materials

The following materials were used for this research work; Alumina powder (Al_2O_3), Silicon carbide powder (SiC), Boron carbide powder (B_4C), Silicon carbide whiskers, Polyvinyl Alcohol (PVA), Polymethyl Methacrylate (PMMA) and Acrylics.

3.2 Equipment

The key equipment used in this study included: X-ray Fluorescence (XRF) for qualitative and quantitative elemental analysis, Energy Dispersive Spectroscopy (EDS) and Scanning Electron Microscopy (SEM) for microstructural and elemental mapping, X-ray Diffraction (XRD) for phase identification, Fourier Transform Infrared Spectroscopy (FTIR) for identifying functional groups, Universal Testing Machine (UTM) for tensile and mechanical testing, Thermal Gravimetric Analyzer (TGA) for thermal stability assessment, Furnace for sample preparation, Weighing balance and molds for composite fabrication.

3.3 Methods

3.3.1 Formulation of composites

The formulation by percentage and weight for Alumina (Al_2O_3), Silicon Carbide (SiC), and Boron Carbide (B_4C) are given in this section.

3.3.1.1 Percentage formulation for Alumina-Silica Carbide

For the Alumina-Silicon Carbide composite preparation, four formulation runs were designed with varying compositions. The alumina content was systematically reduced from 50% to 35%, while maintaining the silicon carbide content constant at 20%. Simultaneously, the whisker content was increased from 10% to 25%, and the binder content was kept steady at 20% across all runs. In terms of weight, each batch was proportioned carefully: Run 1 used 5g alumina, 2g silicon carbide, 1g whiskers, and 2g binder. Subsequent runs adjusted the alumina and whisker amounts incrementally, with Run 2 using 4.5g alumina and 1.5g whiskers, Run 3 using 4g alumina and 2g whiskers, and Run 4 using 3.5g alumina and 2.5g

whiskers, while keeping silicon carbide and binder weights constant at 2g each. These formulations ensured a controlled comparison of how incremental changes in alumina and whisker content influenced the mechanical and microstructural properties of the composites.

3.3.1.3 Percentage Formulation for Alumina-Boron Carbide

For the Alumina-Boron Carbide composites, four formulation runs were developed with controlled variations. The percentage of alumina was reduced stepwise from 50% to 35%, while the boron carbide content was consistently maintained at 20%. At the same time, the whisker content was gradually increased from 10% to 25%, and the binder proportion was held constant at 20% across all runs. In terms of weight, Run 1 consisted of 5g alumina, 2g boron carbide, 1g whiskers, and 2g binder. Run 2 adjusted to 4.5g alumina and 1.5g whiskers; Run 3 used 4g alumina and 2g whiskers; and Run 4 applied 3.5 g alumina and 2.5g whiskers, while keeping the boron carbide and binder weights steady at 2g each. This systematic variation allowed the study to assess the influence of compositional changes on the mechanical strength, stiffness, and ductility of the Alumina-Boron Carbide composites.

3.3.2 Fabrication Process of Alumina-Silicon Carbide and Boron Carbide Composites

The fabrication of alumina (Al_2O_3), silicon carbide (SiC), and boron carbide (B_4C) composites followed a systematic approach to ensure optimal microstructural properties and mechanical performance. The process included the following steps: i. Powder Selection: High-purity powders with the desired particle size distribution were selected for each component (Al_2O_3, SiC, B_4C) to ensure homogeneity and consistency in the final composite. ii. Proportioning: The proportions of each component were determined based on the experimental design to achieve the desired mechanical and thermal properties. iii. Mixing: The powders were thoroughly mixed using a ball mill or other suitable mixing equipment to ensure homogeneous particle distribution. iv. Binder Addition: An acrylic-based binder was added to improve cohesion and aid in the forming process. Forming: The mixture was shaped into the desired form using dry pressing under a controlled pressure environment. Drying: The formed composites were allowed to dry at room temperature to ensure proper curing before sintering. Sintering: The dried composites were subjected to high-temperature sintering at 1200°C to promote particle bonding and densification. Cooling: The sintered composites were cooled using a forced draft fan to minimize thermal stresses and prevent microcrack formation.

3.3.3 Characterization of Alumina-Silicon Carbide and Boron Carbide Composites

A range of techniques was employed to analyze the physical, mechanical, thermal, and chemical properties of the fabricated composites. The characterization focused on morphology, crystallinity, microstructure, functionality, and thermal stability.

3.3.3.1 Morphology, Crystallinity, and Microstructure Analysis

i. X-ray Diffraction (XRD) Analysis

X-ray Diffraction (XRD) was utilized to examine the crystalline structure, phase composition, and degree of crystallinity of the composite materials. The analysis was conducted using a Rigaku Miniflex X-ray Diffractometer with Cr Kα radiation ($\lambda = 2.29$ Å), operated at 40 kV and 40 mA. Samples were finely ground, evenly spread on sample holders, and scanned across 2θ angles ranging from 5° to 80° at a specified step size. The diffraction patterns were analyzed to identify crystalline phases and calculate crystallinity percentages.

ii. Scanning Electron Microscopy (SEM) Analysis

Scanning Electron Microscopy (SEM) was employed to evaluate the microstructure, surface morphology, and fracture behavior of the composites. The samples were cut into cross-sections using a precision cutting blade and coated with a thin platinum layer via plasma sputtering to enhance conductivity. The microstructural features, including particle distribution, porosity, phase dispersion, and fiber-matrix interactions, were examined using a HITACHI S4800 SEM under vacuum conditions. High-resolution images were captured to assess void formation, crack propagation, and agglomeration of reinforcing particles.

3.3.3.2 Functionality and Bond Type Analysis

i. X-ray Fluorescence (XRF) Analysis

X-ray Fluorescence (XRF) spectroscopy was used to determine the elemental composition of the composites, quantifying the concentrations of silicon (Si), aluminum (Al), iron (Fe), calcium (Ca), magnesium (Mg), and other trace elements. Powdered samples were pressed into pellets and analyzed using an XRF spectrometer, which emitted high-energy X-rays to induce fluorescence in the sample. The emitted secondary X-rays were recorded and analyzed to assess mineral purity and composition.

ii. Fourier Transform Infrared Spectroscopy Analysis

Fourier Transform Infrared Spectroscopy (FTIR) was conducted to analyze chemical bonding and functional groups within the composite matrix. Samples were either mixed with potassium bromide (KBr) to form thin pellets or analyzed using ATR-FTIR for direct spectral measurements. The absorption spectra were recorded over a wavelength range of 4000–400 cm^{-1}, identifying characteristic peaks corresponding to hydroxyl (-OH), carbonyl (C=O), silicate (Si-O), and other molecular vibrations. The data provided insights into phase transformations and chemical interactions within the composite.

3.3.3.3 Thermal Stability Analysis using Thermogravimetric Analysis

Thermogravimetric Analysis (TGA) was performed to evaluate the thermal stability and weight loss behavior of the composite materials under high-temperature conditions. Each sample was heated at a rate of 15°C/min under a nitrogen atmosphere for one hour (3600 s). The mass change in the composites was continuously recorded, and a weight loss percentage (ωc %) was calculated using the following equation:

$$w_c\% = \frac{w_{co} - w_{cn}}{w_c} X100\ \% \quad (1)$$

Where: ω_c % = percent weight change in composite, ω_{co} = old weight during testing, ω_{cn} = new weight during testing, ω_c = original weight measured before testing. A weight loss vs. temperature plot was generated to analyze thermal degradation patterns, allowing for the assessment of composite stability and decomposition temperatures.

3.3.4 Optimization of Ceramic Matrix Composite Production Using Design of Experiments

The structural properties, mechanical performance, and overall characteristics of ceramic matrix composites are significantly influenced by factors such as strength, density, and fiber orientation. These factors directly impact the yield of graphene-based reinforcements in security applications. To optimize these parameters, the Taguchi design of experiments (DOE) approach was employed. The primary objective of this optimization process was to achieve a ceramic matrix composite with enhanced ultimate strength while maintaining a low density—critical attributes for security applications. The key processing parameters influencing these performance criteria were identified as mixture composition and processing time. Each of these factors was studied at two distinct levels to determine their optimal configurations. To systematically evaluate the influence of these parameters, a modified L_a (b^c) orthogonal array was selected for the experimental design. This array structure provides an efficient method for assessing multiple factors while minimizing the number of experimental trials. The design parameter control level is shown in Table 1.

Table 1. Design Parameter Control Level

Parameter (units)	Level of Controlling of Design Parameter			
	1	2	3	4
Mix ratio (CP, RM, B) wt%	50:40:10	45:40:15	40:40:20	35:40:25
Time (min)	5	7.5	10	12.5

Where CP = Ceramic Powder, RM = Reinforcement material and B = Binder

The optimization of ceramic matrix composite (CMC) production was performed using a Level 4 Orthogonal Array (OA), which allowed for four experimental runs. Each row in the OA represented a unique combination of factor levels, ensuring a balanced and efficient experimental design. This

approach facilitated the investigation of both main effects and two-way interactions with a minimal number of experimental trials while maintaining statistical robustness [24]. To optimize the mechanical and structural performance of the ceramic matrix composites (CMCs), the manufacturing process employed a high sintering temperature (1200°C) and 5 bar pressure, tailored mold designs, and careful atmosphere control (using vacuum, inert gases, or reducing environments) to prevent oxidation, grain irregularities, and contamination. Protective coatings were sometimes applied for added oxidation resistance. Throughout production, quality control measures—such as monitoring density, porosity, microstructure, and mechanical integrity—were rigorously applied. Finally, the mechanical properties of the developed CMCs were evaluated through tensile strength (ASTM D638), impact strength (ASTM D256), and hardness tests (ASTM E10-18).

4 RESULTS AND DISCUSSION

4.1 Results

The various results obtained during the research work are reflected in tables and figures below.

4.1.1 Characterization of Al_2O_3-SiC and Al_2O_3-B_4C Materials: Thermal Stability, Composition, Microstructure and Bond Analysis

4.1.1.1 Thermogravimetric Analysis (TGA)/Differential thermal Analysis (DTA)

The results obtained for thermogravimetric analysis (TGA/DTA) for Al-Sic and Al-B_4C as shown in Figures 1 through 4.

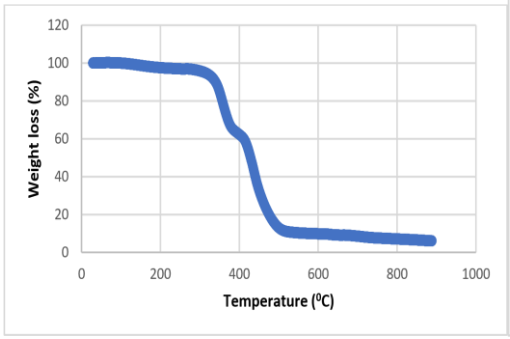

Figure 1. TGA for alumina-silica carbide.

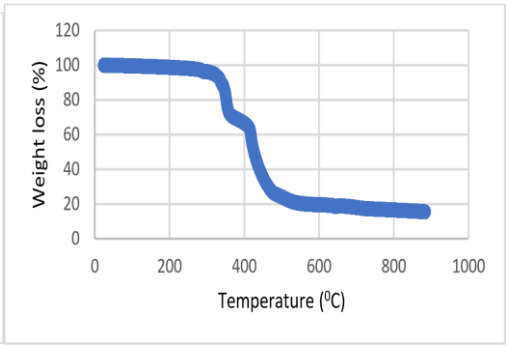

Figure 2. TGA for alumina-boron carbide.

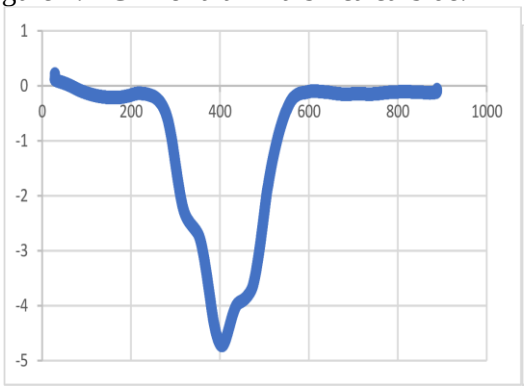

Figure 3. DTA for alumina-silicon carbide.

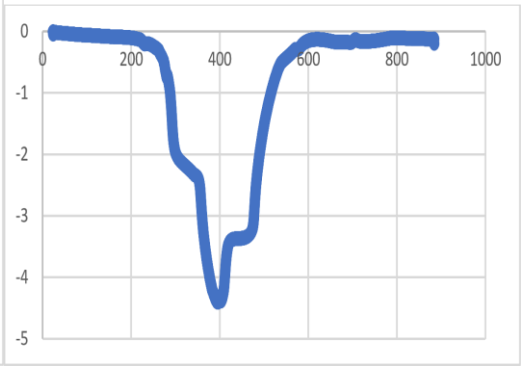

Figure 4. DTA for alumina-boron carbide.

4.1.1.2 X-Ray Diffractometer Analysis

The results obtained for XRD analyzed are shown in Figures 5, 6 and Tables 2, 3.

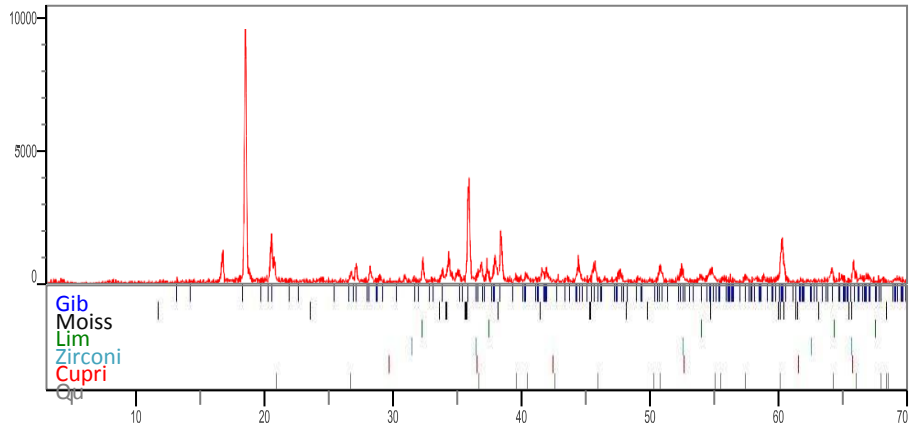

Figure 5. XRD for alumina-silicon carbide

Table 2. XRD for alumina-silicon carbide

No.	**2θ, °**	**d, Å**	**Height, cps**	**FWHM, °**	**Int. I., cps°**
1	16.750(7)	5.289(2)	691(93)	0.179(16)	141(11)
2	18.493(6)	4.7939(14)	6870(286)	0.160(4)	1311(23)
3	20.507(12)	4.327(2)	1116(111)	0.193(15)	337(15)
4	27.095(18)	3.288(2)	209(30)	0.45(6)	105(13)
5	28.157(12)	3.1667(13)	304(61)	0.18(4)	71(9)

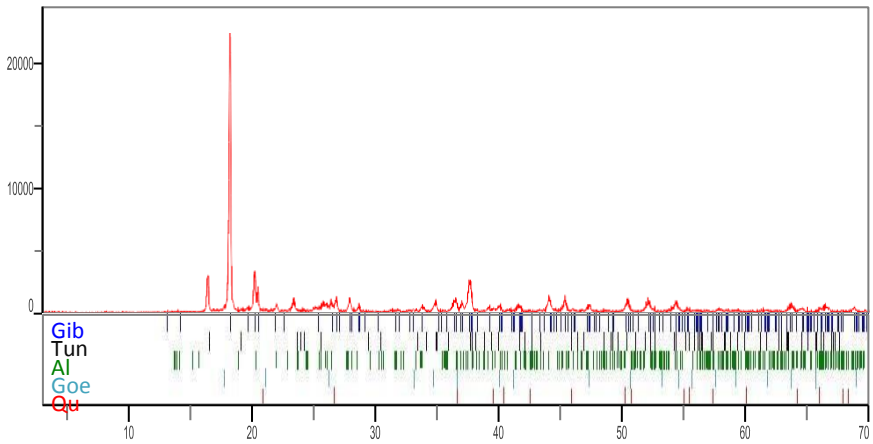

Figure 6. XRD for alumina-boron carbide

Table 3. XRD for Alumina-Boron Carbide

No.	2θ, °	d, Å	Height, cps	FWHM, °	Int. I., cps°	Int. W., °
1	16.423(10)	5.393(3)	2140(155)	0.148(11)	379(11)	0.177(18)
2	18.191(3)	4.8729(8)	16029(435)	0.153(2)	3013(26)	0.188(7)
3	20.183(15)	4.396(3)	2255(158)	0.158(12)	474(28)	0.21(3)
4	20.428(11)	4.344(2)	1099(111)	0.12(2)	181(23)	0.16(4)
5	21.98(4)	4.040(8)	290(42)	0.18(3)	57(10)	0.20(6)

4.1.1.3 X-Ray Fluorescence

The results of XRF analysis for Aluminum Silicon Carbide and Aluminum Boron Carbide are shown in Figure 7.

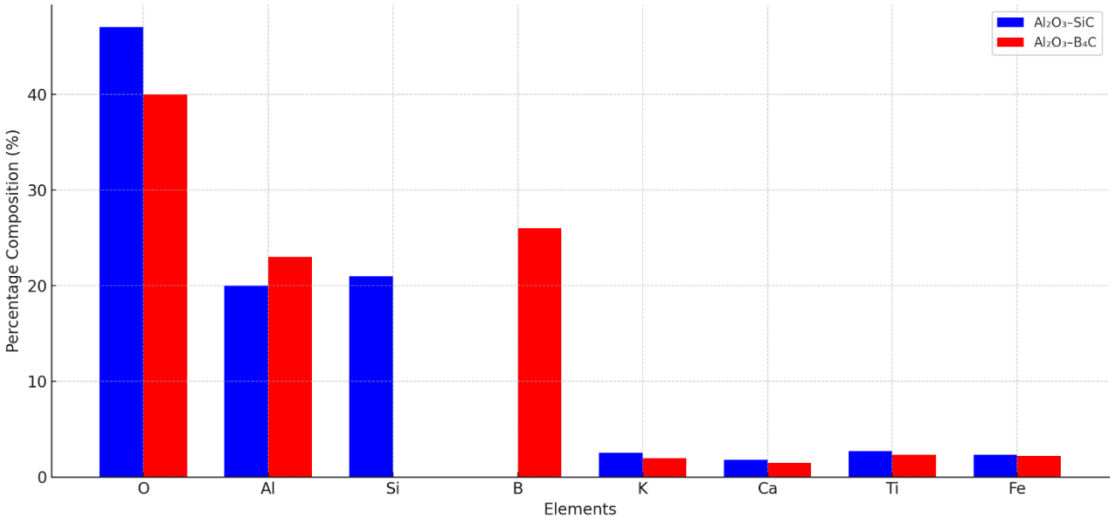

Figure 7. Combined XRF Plot (**blue** for **SiC composite** and **red** for **B_4C composite)**

4.1.1.4 Fourier's Transform infrared spectroscopy

The results of FTIR analysis for aluminum silicon carbide and aluminum boron carbide are shown in Figures 8 and 9 respectively.

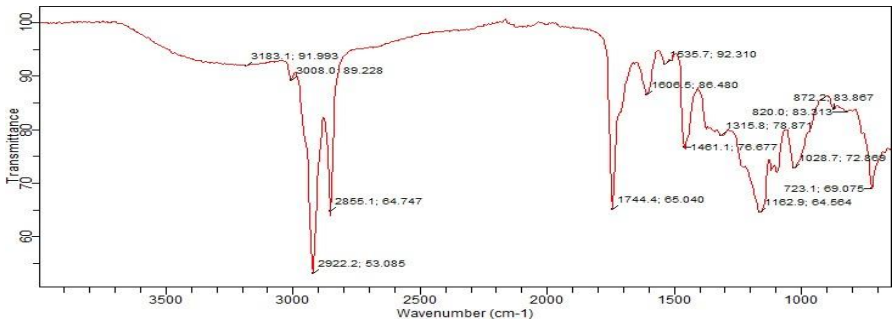

Figure 8. FTIR for Alumina-Silicon Carbide

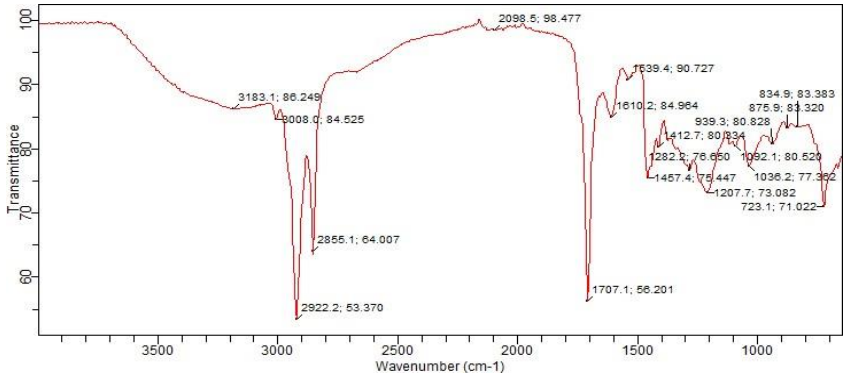

Figure 9: FTIR for Alumina-Boron Carbide

4.1.1.5 Scanning Electron Microscope

The SEM results obtained for the alumina-silicon carbide and alumina-boron carbide are shown below in Plates 1 and 2.

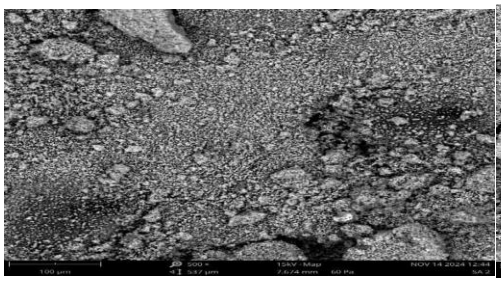

Plate 1. SEM for alumina-silicon carbide

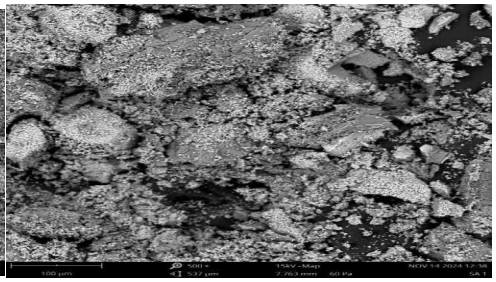

Plate 2. SEM for alumina-boron carbide

4.1.1.6 Energy Disperse Spectroscopy

The results of energy disperse spectroscopy for both are shown in Table 4.

Table 4. Combined EDS Values

Element	Symbol	Atomic Conc. (%) (SiC)	Weight Conc. (%) (SiC)	Atomic Conc. (%) (B_4C)	Weight Conc. (%) (B_4C)
Aluminum	Al	53.42	46.97	49.76	51.53
Silicon	Si	37.74	43.74	—	—
Boron	B	—	—	23.86	28.34
Oxygen	O	1.96	2.22	5.55	3.32
Carbon	C	1.93	1.85	4.73	5.54
Calcium	Ca	1.47	1.46	6.77	4.3
Magnesium	Mg	1	1.42	4.07	2.53
Phosphorus	P	1.56	1.34	1.32	1.92
Potassium	K	0.92	1.01	0.88	0.98

4.1.2 Optimization of Ceramic Matrix Composite (CMC) Production Using Taguchi

The optimization of the ceramic matrix composite (CMC) production process using the Taguchi orthogonal array method analyzed the effects of mix ratio, time, and temperature on composite properties, where the mix ratio (proportions of ceramic powder, reinforcement material, and binder in weight percentage) were varied across four levels (50:40:10, 45:40:15, 40:40:20, 35:40:25), time was controlled at four levels (5, 7.5, 10, and 12.5 minutes).

4.2 Discussion of Results

The various results obtained in this research work are hereby discussed accordingly

4.2.1 Characterization

The Thermogravimetric Analysis (TGA) of the Alumina-Silicon Carbide (Al_2O_3-SiC) composite (Figure 1) indicates initial thermal stability between 25–50°C, followed by a stable region up to 200°C. Gradual weight loss from 200–400°C corresponds to the decomposition of organic binders, while the sharp drop between 400–600°C is attributed to carbon compound breakdown and the oxidation of SiC to SiO_2 and CO_2. From 600–800°C, the curve stabilizes, suggesting the presence of thermally robust ceramic phases. The plateau from 800–1000°C confirms the material's high thermal stability, reinforcing its suitability for applications such as refractories, structural components, wear-resistant coatings, and body armor. Differential Thermal Analysis (DTA) of the Al_2O_3-SiC composite (Figure 3) reflects corresponding thermal events: a minimal energy change up to 200°C (moisture loss), a gradual endothermic reaction from 200–400°C (binder decomposition), and a sharp exothermic peak between 400–600°C due to SiC oxidation. The thermal curve stabilizes from 600–800°C and remains unchanged up to 1000°C, confirming the composite's structural integrity and thermal resilience. The TGA profile for the Alumina-Boron Carbide (Al_2O_3-B_4C) composite (Figure 2) shows initial weight stability from 0–200°C due to moisture evaporation, followed by binder and impurity decomposition between 200–400°C. A sharp weight loss from 400–600°C reflects B_4C oxidation into boron oxide (B_2O_3), CO, and CO_2, accompanied by

microstructural transitions. Stabilization between 600–800 °C and negligible change beyond 800°C affirm the composite's thermal stability for high-performance armor applications. DTA results for the Al_2O_3-B_4C composite (Figure 4) support the TGA findings: moisture loss below 200°C, endothermic decomposition from 200–400 °C, and a prominent exothermic peak from 400–600°C attributed to B_4C oxidation. Thermal stabilization beyond 600 °C reflects the formation of durable ceramic phases, reinforcing its applicability in refractory and protective systems. X-ray Diffraction (XRD) analysis of the Al_2O_3-SiC composite (Figure 5, Table 2) shows well-defined peaks for Alumina (25–35° 2θ) and SiC (35–45° 2θ). Peak sharpness and intensity denote high crystallinity and phase purity. Peaks at 16.750°, 18.493°, and 20.507° indicate well-ordered structures, while broader peaks at 27.095° and 28.157° suggest secondary phases or slight disorder—attributes conducive to high thermal and mechanical performance. The XRD spectrum for the Al_2O_3-B_4C composite (Figure 6, Table 3) reveals prominent peaks at 16.423°, 18.191°, and 20.183°, indicating moderate to strong crystallinity. The intense peak at 18.191° particularly affirms a highly crystalline phase. Broader peaks at 20.428° and 21.980° suggest secondary structural variations. These features make the composite ideal for applications demanding structural order and high hardness. X-ray Fluorescence (XRF) data (Figure 7) confirm the elemental compositions of the composites. Al_2O_3-SiC comprises approximately 47% oxygen, 20% aluminum, and 21% silicon, consistent with alumina and silicon carbide phases. Minor elements (e.g., Ca, Ti, Fe, K) may function as sintering aids or introduce secondary phase formation. Al_2O_3-B_4C contains 40% oxygen and 23% aluminum, confirming its alumina base, with 26% bromine suggesting boron-based compounds, potentially Boron Carbide. Trace impurities may influence microstructural behavior. Fourier Transform Infrared (FTIR) analysis (Figures 8 and 9) identifies key functional groups. For Al_2O_3-SiC (Figure 8), O–H stretching (~3183 cm^{-1}), C–H (~2922 cm^{-1}), and C=O (~1744 cm^{-1}) peaks suggest moisture and organic residues. Si–O–Si (~1000–1200 cm^{-1}), Al–O (~723 cm^{-1}), and Si–C (~820 cm^{-1}) vibrations confirm composite bonding and matrix structure. For Al_2O_3-B_4C (Figure 9), O–H, B–H (~2098 cm^{-1}), B–C (~875–870 cm^{-1}), and B–O–Si (~1200–1000 cm^{-1}) signals support the presence of boron carbide and alumina phases. Scanning Electron Microscopy (SEM) analysis (Plates I and II) reveals significant microstructural differences. Al_2O_3-SiC (Plate I) shows uniform grain dispersion, dense packing, and tight bonding with porosity <1 μm, favoring thermal and mechanical strength. However, intergranular fractures and iron contamination (from EDS) suggest a need for improved processing to reduce brittleness and enhance corrosion resistance. Al_2O_3-B_4C (Plate II) displays heterogeneous particle dispersion, rougher morphology, and agglomeration, contributing to enhanced mechanical interlocking but potential structural inhomogeneity. Energy Dispersive X-ray Spectroscopy (EDS) results (Table 4) confirm elemental distributions. Al_2O_3-SiC exhibits high aluminum (53.42 at.%) and silicon (37.74 at.%) content, with trace oxygen and carbon verifying alumina and silicon carbide phases. Minor elements (Ca, Mg, P, K) may act as sintering additives or impurities. In Al_2O_3-B_4C, aluminum (49.76 at.%), boron (23.86 at.%), and carbon (4.73 at.%) indicate a robust boron carbide-alumina matrix with moderate oxygen levels and trace additives, suitable for high-strength, high-temperature applications.

4.2.2 Optimization

The Taguchi orthogonal array method optimized the ceramic matrix composite (CMC) production by analyzing the effects of mix ratio, time, and temperature. Mix ratios (50:40:10 to 35:40:25), processing times (5–12.5 min), and temperature variations were tested using an L16 array. Performance metrics (hardness, tensile strength, density) were evaluated via Signal-to-Noise (S/N) analysis, identifying optimal parameters while minimizing experimental effort and costs, ensuring an efficient, tailored production process.

4.2.3 Mechanical Properties

4.2.3.1 Tensile Test

The tensile behavior of the developed composites was examined under controlled load conditions to assess their stiffness, strength, ductility, and fracture characteristics. Results are shown in Figures 10–17.

Run 1 – Al_2O_3–SiC Composite: This sample demonstrated high stiffness with an elastic modulus of 1243.80 MPa, signifying strong resistance to elastic deformation. A yield strength of 86.10 MPa and ultimate tensile strength (UTS) of 89.00 MPa suggest modest load-bearing capacity. The yield ratio of 96.74% reflects limited plastic deformation prior to fracture—ideal for ceramics in armor that are intended to absorb impact energy through brittle failure [4]. Its low elongation of 5.23% confirms brittleness, while a proof stress of 79.70 MPa and maximum load of 3.56 kN indicate utility in rigid ballistic applications (Figure 10).

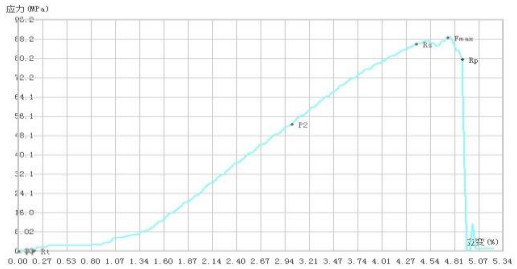

Figure 10. Tensile test for R1 (50:20:10:20) alumina silicon carbide

Run 2 – Al_2O_3–SiC Composite: This configuration showed lower modulus (1051.47 MPa) but significantly improved tensile strength (116.90 MPa) and elongation (12.29%)**,** suggesting enhanced ductility and energy dissipation. A yield ratio of 68.61% reflects pronounced plastic deformation prior to failure, making it suitable for components that absorb and redistribute energy under load [18]. Despite a peak load of 4.68 kN, the low break strength (0.70 MPa) suggests diminished structural reliability post-failure (Figure 11)**.**

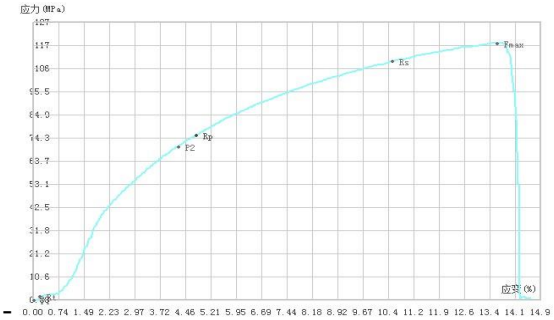

Figure 11. Tensile test for R2 (45:20:15:20) alumina-silicon carbide

Run 3 – Al_2O_3–SiC Composite: Balanced mechanical properties were observed, with elastic modulus of 1152.94 MPa**,** yield strength of 109.60 MPa**,** and UTS of 117.80 MPa**.** The yield ratio (93.04%) **and** elongation of 14.58% suggest excellent compromise between strength and ductility. A peak load **of** 4.71 kN and low break strength (0.40 MPa) point to energy-absorbing potential without substantial residual load capacity (Figure 12).

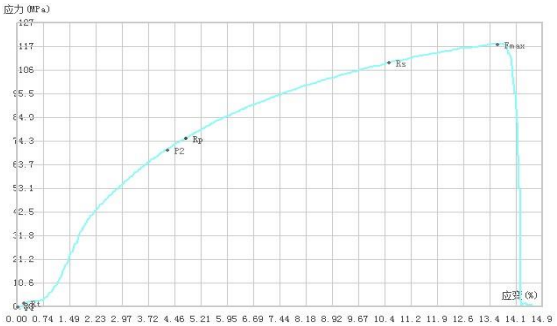

Figure 12. Tensile test for R3 (40:20:20:20) alumina-silicon carbide

Run 4 – Al_2O_3–SiC Composite: This sample showed elastic modulus of 1044.44 MPa**,** yield strength of 61.20 MPa**,** and UTS of 77.90 MPa**.** The elongation (5.44%)**,** yield ratio (78.56%)**,** and full reduction in area (100%) indicate controlled ductile fracture. With proof stress of 66.30 MPa and break strength of 2.80 MPa**,** the composite appears suitable for moderate structural and ballistic roles (Figure 13).

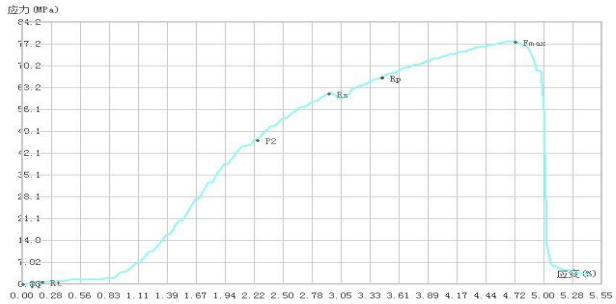

Figure 13. Tensile test for R4 (35:20:25:20) alumina-silicon carbide

Run 1 – Al_2O_3–B_4C Composite: This composite exhibited high stiffness (1301.89 MPa)**,** moderate tensile strength (81.10 MPa)**,** and low ductility (4.72%)**.** The negligible strain hardening and brittle failure characteristics align with its use in armor systems designed to shatter on impact, absorbing energy efficiently [19]. A maximum load of 3.24 kN and proof stress of 74.70 MPa confirm its role in rigid, moderate-impact defense layers (Figure 14).

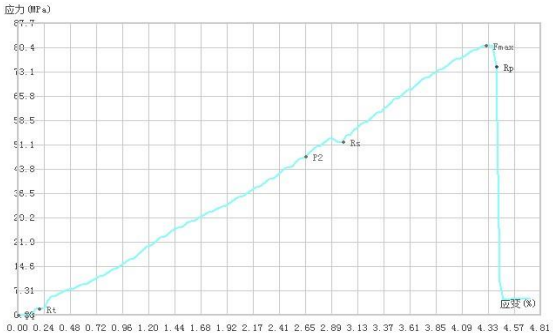

Figure 14. Tensile test for R1 (50:20:10:20) alumina-boron carbide

Run 2 – Al_2O_3–B_4C Composite: Though stiffness was high (1359.92 MPa)**,** the extremely low yield strength (15.79 MPa) limits its structural applications. Nonetheless, with elongation of 5.41% and UTS of 62.56 MPa**,** it could be viable in low-stress or multi-layered armor systems where energy dispersion outweighs peak strength (Figure 15).

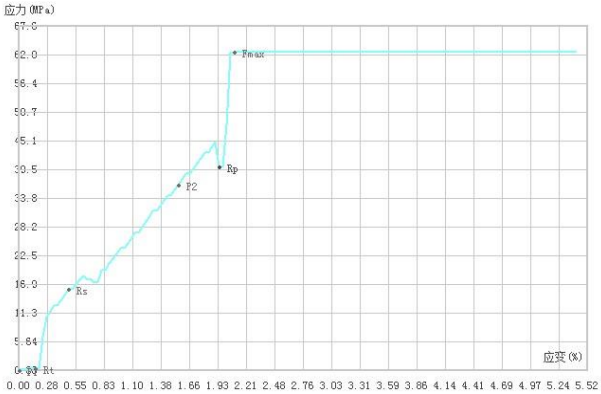

Figure 15. Tensile test for R2 (45:20:15:20) alumina-boron carbide

Run 3 – Al_2O_3–B_4C Composite: This sample recorded the highest stiffness (1461.54 MPa) among all tested samples. Coupled with yield strength of 71.70 MPa**,** UTS of 102.30 MPa**,** and ductility of 7.18%**,** it presents a balanced profile suitable for light to medium ballistic applications. A proof stress of 90.10 MPa and break strength of 0.80 MPa indicate good strength-to-weight performance (Figure 16)**.**

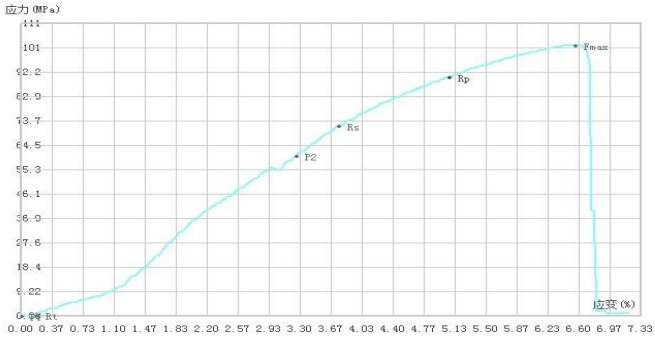

Figure 16. Tensile test for R3 (35:20:25:20) alumina-boron carbide

Run 4 – Al_2O_3–B_4C Composite: This specimen displayed moderate stiffness (1098.77 MPa) and strength (yield: 58.20 MPa), with elongation of 5.60%**,** suggesting some degree of impact energy absorption. Although brittle (break strength: 0.90 MPa), its mechanical profile supports complementary use in layered armor designs (Figure 17)**.**

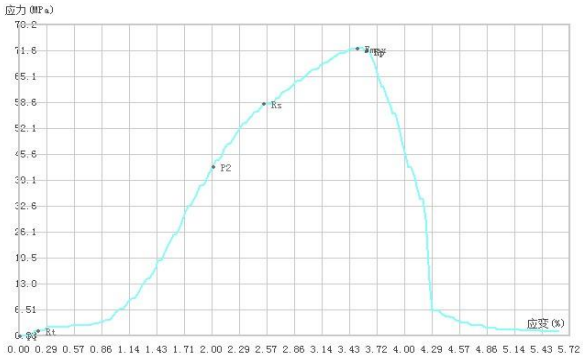

Figure 17. Tensile test for R4 (40:20:20:20) alumina-boron carbide

4.2.3.2 Hardness Test

*Al_2O_3–SiC Composites***:** Brinell hardness values ranging from 9.20–9.40 HRB were recorded. Although lower than standard armor ceramics (typically >500 HB) [14], this composite is effective as a backing or structural layer in hybrid armor configurations, providing post-impact rigidity and energy redistribution (Figure 18)**.**

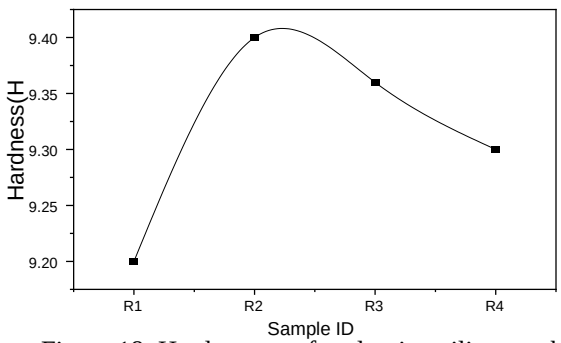

Figure 18: Hardness test for alumina-silicon carbide

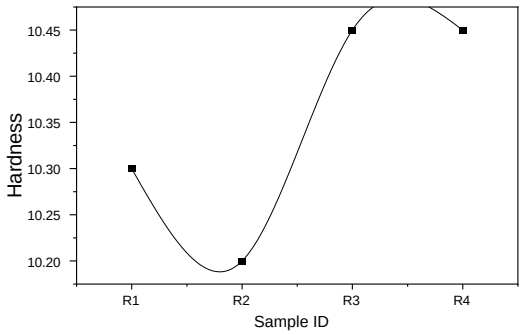

Figure 19. Hardness test for alumina-boron carbide

Al_2O_3–B_4C Composites: Hardness values between 10.20–10.45 HRB indicate slightly better resistance to localized plastic deformation (Figure 19). While still below ballistic-grade hardness benchmarks, these composites may serve effectively as intermediate or structural layers, particularly when lightweight is critical [15].

4.2.3.3 Impact Test

*Al_2O_3–SiC Composites***:** Impact absorption ranged from 5.30 to 5.60 J**,** signifying limited shock resistance due to the brittle nature of the matrix. These materials are not ideal as strike-face components but perform well in spall-limiting or reinforcing layers (Figure 20)**.**

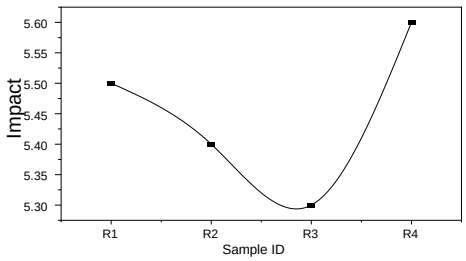

Figure 20. Impact test for alumina-silicon carbide

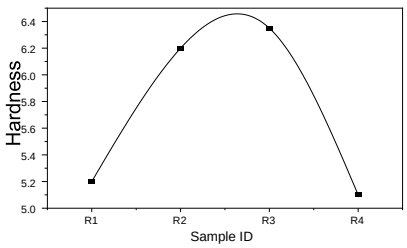

Figure 21. Impact test for alumina-boron carbide

Al_2O_3–B_4C Composites: These samples showed slightly higher impact energy absorption **(**5.10–6.35 J**),** reinforcing their utility in multilayer **systems** where penetration resistance and shock dispersion are critical (Figure 21)**.** Their superior stiffness and moderate ductility enhance their ballistic compatibility when paired with ductile substrates [20].

4.2.4 Comparative Study and Performance Evaluation of Developed Composites

Ceramic-reinforced composites are integral to modern ballistic and body armor applications due to their outstanding hardness, stiffness, and capacity for energy absorption [21, 22]. In this study, a comparative evaluation was carried out between Alumina–Silicon Carbide (Al_2O_3–SiC) **and** Alumina–Boron Carbide (Al_2O_3–B_4C) composites to assess their mechanical characteristics and suitability for ballistic protection systems.

4.2.4.1 Hardness and Ballistic Resistance

The hardness of a composite directly influences its resistance to penetration by high-velocity projectiles [23]. Al_2O_3–SiC composites exhibited lower hardness values, ranging from 9.20 to 9.40 HRB**,** suggesting limited efficiency as a standalone strike-face material. Nevertheless, these composites may serve effectively in backing or structural layers within multi-layered armor systems where energy distribution is critical. In contrast, Al_2O_3–B_4C samples demonstrated superior hardness values between 10.20 and 10.45 HRB**,** indicating stronger potential for serving as the primary strike-face layer, capable of disrupting and absorbing high-velocity impacts.

4.2.4.2 Impact Energy Absorption

Al_2O_3–SiC composites absorbed between 5.30 and 5.60 J of impact energy, reflecting moderate shock absorption performance. While useful in mitigating secondary impacts, this range may not suffice under direct high-velocity ballistic loads. Al_2O_3–B_4C composites, however, exhibited marginally higher energy absorption capacities of **5.10 to 6.35 J**, reinforcing their candidacy for primary ballistic applications where both hardness and energy dissipation are required [19].

4.3.4.3 Suitability for Ballistic Application

From the above analyses, Al_2O_3–SiC is deemed more suitable for hybrid or multi-layer armor systems where its primary function would involve spall reduction and structural integrity. On the other

hand, Al_2O_3–B_4C possesses the hardness and energy management capabilities to serve as the first line of defense, absorbing the brunt of high-energy projectiles.

4.2.4.4 Optimization via Taguchi Method

Using the Taguchi design of experiments, the influence of processing parameters such as mix ratio, sintering time, and temperature was statistically assessed. Results showed that optimization significantly improved material densification and interfacial bonding. Notably, only the Al_2O_3–B_4C composites met the critical thresholds for use in primary ballistic protection**,** in line with previous optimization studies [24]. Mechanical Property Summary: Elastic Modulus**:** The Al_2O_3–B_4C composites attained a higher modulus (up to 1461.54 MPa**)**, indicating increased rigidity and better resistance to elastic deformation. Yield Strength: Al_2O_3–SiC exhibited superior yield strength **(**up to 109.60 MPa**),** suggesting greater resistance to initial plastic deformation under load. Tensile Strength**:** The highest tensile strength was observed in Al_2O_3–SiC composites **(**up to 117.80 MPa**),** implying better suitability for structural or load-bearing applications where ductility and toughness are required.

4.2.4.5 Application Relevance

Based on the mechanical and ballistic characteristics: Al_2O_3–SiC is ideal for use in hybrid armor systems**,** especially as a secondary or support layer that enhances impact absorption and load distribution. Al_2O_3–B_4C is most effective as the primary shielding material, providing the hardness and energy dissipation necessary to stop or reduce the penetration of projectiles at high velocities.

5 CONCLUSIONS

This study successfully developed and characterized Al_2O_3-SiC and Al_2O_3-B_4C ceramic composites for ballistic applications. Thermal, structural, and mechanical evaluations revealed that while Al_2O_3-SiC offers superior tensile strength and ductility, its lower hardness limits standalone application in ballistic protection. In contrast, Al_2O_3-B_4C exhibited higher hardness, stiffness, and energy absorption, making it a more effective primary armor material. The use of Taguchi optimization enhanced composite performance, confirming that processing parameters critically influence strength and impact resistance. Overall, Al_2O_3-B_4C is better suited for high-velocity ballistic protection, while Al_2O_3-SiC serves well in support or hybrid armor systems.

REFERENCES

1. Tella, C.M. (2015). Insecurity in Northern Nigeria: Causes, Consequences and Resolutions. *International Journal of Peace and Conflict Studies*, vol. 2, no. 4, pp. 23-36.
2. Baldwin, D.A. (1997). The Concept of Security. *British International Studies Association*.
3. Emmanuel, I.O., Emily, O.A. (2019). Insecurity Crisis in Nigeria: The Law Enforcement Agents a Panacea. *Journal of Sociology and Social Work*, vol. 7, no. 1, pp. 44-57.
4. Cantwell, W.J. and Morton, J. (1991). The Impact Resistance of Composite Materials -- A Review. *Composites*, vol. 22, no. 5, pp. 347-62.
5. Boccaccini A.R., Atiq, S., Boccaccini, D.N., Dlouhy, I. and Kaya, C. (2005). Fracture Behaviour of Mullite Fibre Reinforced-Mullite Matrix Composites Under Quasi-Static and Ballistic Impact Loading. *Composites Science and Technology*, vol. 65, no. 2, pp. 325-333.
6. Definition of Armour in English (2012). Oxford Dictionaries. Archived from the original on 29 July (2012). Retrieved 12 April (2016).
7. Nepal, D., Kang, S., Adstedt, K.M., Kanhaiya, K., Bockstaller, M.R., Brinson, L.C., Buehler, M.J., Coveney, P.V., Dayal, K., El-Awady, J.A., Henderson, L., Kaplan, D, L., Keten, S., Kotov, N.A. and Schatz, G.C. (2022). Hierarchically Structured Bioinspired Nanocomposites. *Nature Materials*, vol. 22, no. 1, pp. 18-35.

8. McEvoy, M.A. and Correll, N. (2015). Materials that Couple Sensing, Actuation, Computation, and Communication. Science, vol. 347, no. 6228): 1261689.
9. L. Special Furnace; Aston, Inc 20 Kent Road; Pa 19014 877.846.7628 (2018). What are Ceramic Matrix Composites?. L&L Special Furnace Co, Inc. Archived from the original on 2020-09-28. Retrieved 2020-12-17.
10. Zoli, L. and Sciti, D. (2017). Efficacy of a ZrB 2 –SiC matrix in protecting C fibres from oxidation in novel UHTCMC materials. *Materials & Design*, vol. 113, pp. 207-213.
11. Alumina the Different Types of Commercially Available Grades (2007). The A to Z of Materials. 3 May 2002. Archived from the original on 10 October 2007. Retrieved 27 October 2007.
12. Zoli, L. and Sciti, D. (2017). Efficacy of a ZrB 2 –SiC Matrix in Protecting C Fibres from Oxidation in Novel UHTCMC Materials. *Materials & Design*, vol. 113, pp. 207-213.
13. Zoli, L., Vinci, A., Silvestroni, L., Sciti, D., Reece, M. and Grasso, S. (2017). Rapid Spark Plasma Sintering to Produce Dense UHTCs Reinforced with Undamaged Carbon Fibres. *Materials & Design*, vol. 130, pp. 1-7.
14. Medvedovski, E. (2006). Lightweight Ceramic Composite Armour System. *Advances in Applied Ceramics*, vol. 105, pp. 241-245.
15. Halil, K., Şener, K. and Ramazan, Ç. (2018). Study on Mechanical and Ballistic Performances of Boron Carbide Reinforced Al 6061 Aluminum Alloy Produced by Powder Metallurgy. *Composites Part B: Engineering*, vol. 148, pp. 68-80.
16. Olawale, S., Oyelaran, O. and Badmus, J. (2020). Ballistic Study of Alumina Ceramic-Steel Composite for Structural Applications. *Journal of Ceramic Processing Research*, vol. 21, pp. 501-507.
17. Rathod, S., Tiwari, G. and Dilip, C. (2021). Ballistic performance of ceramic–metal composite structures. *Materials Today: Proceedings*, vol. 41, no. 5, pp. 1125-1129.
18. Shahid, M., Malik, R.A., Alrobei, H., Jaehwan, K., Latif, M., Hussain, A., Iqbal, M. and Hafiz, A. (2021). Synthesis and Mechanical Characterization of Alumina Based Composite Material for Amour Application. *Journal of Ceramic Processing Research*, 22p.
19. Zhou, X., Li, Z. and Wang, R. (2018). Impact energy absorption in multi-layer ceramic armors. *International Journal of Impact Engineering*, vol. 118, pp. 112-123.
20. Saurab, R., Tiwari, G. and Dilip, C. (2021). Ballistic performance of ceramic–metal composite structures. *Materials Today: Proceedings*, vol. 41, no. 5, pp. 1125-1129.
21. Lee, W., Zhang, S. and Kim, H. (2020). *Ballistic performance of ceramic matrix composites for armor applications*. ***Journal of the European Ceramic Society***, vol. 40, no. 8, pp. 2873-2882.
22. Menna, C., Asprone, D. and Auricchio, F. (2017). *Materials for lightweight armour: a review on ceramic and polymeric composites*. ***Composites Part B: Engineering***, vol. 118, pp. 96-109.
23. Sørensen, L., Hansen, J. and Nielsen, T. (2021). *Advanced ceramic armour materials: A comparative study of impact resistance*. ***Materials & Design***, 204, 109632.
24. Singh, R., Kumar, A. and Sharma, P. (2019). *Optimization of mechanical behavior in ceramic-metal composites using Taguchi method*. ***Materials Today: Proceedings***, vol. 18, no. 1, pp. 476-483.